Annals of Nuclear Energy 197 (2024) 110249

Contents lists available at ScienceDirect

Annals of Nuclear Energy

journal homepage: www.elsevier.com/locate/anucene

Towards modelling defective fuel rods in TRANSURANUS: Benchmark and assessment of gaseous and volatile radioactive fission product release

L. Giaccardi [a], M. Cherubini [a], G. Zullo [b], D. Pizzocri [b], A. Magni [b], L. Luzzi [b,*]

[a] Nuclear and INdustrial Engineering (NINE), Via della Chiesa XXXIII 759, 55100, Lucca, Italy
[b] Politecnico di Milano, Department of Energy, Nuclear Engineering Division, Via La Masa 34, 20156, Milan, Italy

ARTICLE INFO

Keywords:
Defective fuel rods
Radioactive fission products
Release from fuel to coolant
TRANSURANUS
SCIANTIX

ABSTRACT

This work presents the results of a collaborative benchmark activity between different organizations towards the use of the TRANSURANUS code to estimate the release of gaseous and volatile radioactive fission products from defective fuel rods, into the primary coolant of pressurized water reactors. First, the radioactive release from the fuel to the gap is evaluated according to three approaches: the coupling between TRANSURANUS and SCIANTIX, the development of TRANSURANUS devoted subroutines, and the use of the ANS 5.4–2010 methodology. Fuel-to-gap release calculations are benchmarked and assessed against measured data from the CONTACT1 irradiation experiment. Then, TRANSURANUS has been used to estimate the radioactive release into the primary coolant by applying a first-order phenomenological rate theory and tested against measured data of fission product coolant concentrations from irradiation experiments of the CRUSIFON program.

1. Introduction

During the operation of a nuclear reactor, radioactive fission products (FPs) accumulate within the fuel rods. Most FPs are retained within the fuel pellets. A small, yet not negligible, amount of gaseous and volatile FPs is released from the fuel and accumulated in the fuel rod free volume by recoil, knockout, and diffusion mechanisms (Dong et al., 2019). The fuel rod cladding acts as a first protective barrier against the release of gaseous and volatile radioactive FPs into the coolant (Saad et al., 2021). Also, a low rate of cladding failure events is recognized from past experiences (Locke, 1972; Kim, 2009; Veshchunov, 2019), nevertheless the consequences have shown to be significant (IAEA, 2015). Therefore, accurate predictions of the coolant activity improve the reactor safety. When a defect in the cladding of a light water reactor (LWR) is formed, high-pressure water enters the gap. Radioactive gaseous and volatile FPs escape then into the coolant and increase the coolant activity. Besides, fuel oxidation due to fuel-steam interaction occurs, resulting in a larger radioactive release from the fuel (Massih, 2018) and cladding oxidation acts as a source of hydrogen in the fuel rod free volume, besides radiolysis and steam dissociation, that should be accounted due to potential chemical interactions (Lewis et al., 1990; Lewis, 1990).

Improving current fuel performance codes (FPCs) capabilities to evaluate the radioactive release from the fuel, the gap activity, and the reactor source term is one of the main objectives of the R2CA H2020 European Project (R2CA, 2019). In this regard, the present work involved collaboration between the partners (Politecnico di Milano (PoliMi), NINE (NINE), and JRC-Ka (JRC-Ka) to undertake a TRANSURANUS (Lassmann, 1992; Magni et al., 2021) code development activity towards the modelling of defective fuel rods and the subsequent assessment and benchmarking strategy of the results (Zullo et al., 2023a; Zullo et al., 2023b). To enable the TRANSURANUS code to model the radioactive release from defective fuel rods, models are available in the literature (Veshchunov, 2019; Lewis et al., 2017). The first step is to reproduce the fuel-to-gap release, then, the gap-to-coolant release.

The fuel-to-gap release concerns the transport of radioactive (short-lived) gaseous and volatile FPs from the fuel into the fuel rod free volume. This is considered in the TRANSURANUS fuel performance code according to three different approaches. Namely, (i) the use of the meso-scale code SCIANTIX, developed at Politecnico di Milano (Pizzocri et al., 2020; Zullo et al., 2023c), coupled to TRANSURANUS, (ii) the development of new TRANSURANUS subroutines, performed at NINE, and

* Corresponding author.
E-mail address: lelio.luzzi@polimi.it (L. Luzzi).

https://doi.org/10.1016/j.anucene.2023.110249
Received 11 April 2023; Received in revised form 4 September 2023; Accepted 15 November 2023
Available online 23 November 2023
0306-4549/© 2023 The Authors. Published by Elsevier Ltd. This is an open access article under the CC BY license (http://creativecommons.org/licenses/by/4.0/).

(iii) the application of the recently implemented ANS 5.4–2010 semi-empirical methodology (Turnbull and Beyer, 2010). Fuel-to-gap release calculations are then benchmarked and assessed against the CONTACT1 experiment (Bruet et al., 1980; Charles et al., 1983).

The second step considers the release of FPs from the gap to the coolant, carried out at NINE. This is based on a phenomenological first-order kinetic model (Veshchunov, 2019; Yang-Hyun et al., 1994) that has been implemented in TRANSURANUS. Gap-to-coolant release calculations has been tested against the CRUSIFON1bis and CRUSIFON2 experimental tests (Harrer et al., 1980; Harrer et al., 1981). Further advancement of this work is to consider axial mass transport processes in the gap, e.g., based on the generalized Lewis model (Lewis, 1990).

This paper is organized as follows. In Section 2, two fuel-to-gap modelling approaches (TRANSURANUS//SCIANTIX and TRANSURANUS-NINE) are described, benchmarked, and assessed. In Section 3, the gap-to-coolant model implemented in TRANSURANUS-NINE is outlined, together with the results of CRUSIFON simulations. Conclusions are drawn in Section 4.

2. Model benchmark for the release of radioactive gases to the fuel-cladding gap

The release of fission gases (FGs) and volatile FPs from the fuel to the fuel-cladding gap is attributable to recoil, knockout, and diffusion mechanisms (Lewis, 1988). Under LWR operating conditions, the temperatures reached by the fuel allow disregarding recoil and knockout mechanisms while focusing only on the dominant diffusion mechanism (Dong et al., 2019; Lewis and Husain, 2003). The diffusion of FGs and volatile FPs includes the production within UO_2 grains, diffusion towards grain boundaries and accumulation in grain-boundary bubbles, together with the radioactive decay in the case of unstable isotopes. Bubble growth and coalescence processes result in the grain-boundary bubble interconnection phenomenon which initiates the release of gaseous and volatile FPs from the fuel to the gap (Pizzocri et al., 2020; Booth, 1957; Kogai, 1997; Olander, 1976; Pastore et al., 2013; Rest and Gehl, 1980; Tonks et al., 2018; White and Tucker, 1983; Zullo et al., 2022b; Van Uffelen et al., 2010).

The next section details two mechanistic formulations that describe the behaviour of gaseous and volatile radioactive FPs within the fuel: the model currently implemented in the SCIANTIX code (Pizzocri et al., 2020; Zullo et al., 2022b; Zullo et al., 2022c), automatically inherited by TRANSURANUS via the coupling with SCIANTIX (i.e., TRANSURANUS//SCIANTIX), and the model implemented in the TRANSURANUS code at NINE (i.e., the TRANSURANUS-NINE version). The two formulations are benchmarked and assessed against the CONTACT1 irradiation test (Bruet et al., 1980; Charles et al., 1983). Along with these two physically grounded descriptions, the comparison includes the prediction of TRANSURANUS (in terms of radioactive release-to-birth ratio) when using the semiempirical ANS 5.4–2010, that is fully described in Ref. (Turnbull and Beyer, 2010) and has been recently implemented in the TRANSURANUS code at FORTUM (Zullo et al., 2022c).

2.1. Fuel-to-gap model for the release of radioactive gas in TRANSURANUS//SCIANTIX

The phenomenon of FG release from the fuel to the rod free volume is currently modelled in SCIANTIX (Pizzocri et al., 2020) with a two-step process (Pastore et al., 2013; White and Tucker, 1983; Zullo et al., 2022b; Pizzocri, 2018):

1. FG atoms are uniformly generated within the fuel grains due to fission events. The dominant gas transport mechanism from the fuel to the rod free volume is the atomic diffusion (White and Tucker, 1983; Pastore et al., 2013; Friskney and Speight, 1976; White, 2004; Turnbull et al., 1982; Turnbull et al., 1988), in the first place from within the grains to the grain boundaries, where the gas accumulates in grain-boundary bubbles.
2. The inter-granular bubbles grow by absorption of both FG and vacancies and can coalesce together, resulting in larger and fewer bubbles (White, 2004; Veshchunov, 2008). Coherently with the state-of-the-art modelling (White and Tucker, 1983; Pastore et al., 2013; White, 2004). we assume that this process continues until the grain boundaries are sufficiently populated with large bubbles, and a network of interconnected bubbles is formed. This network constitutes a pathway through which fission gas is vented out of the fuel pellet, as soon as the network gets in touch with an easy escape route, e.g., a fuel crack. We assume that this release happens instantly, i.e., the gas is brought from the grain boundaries to the fuel rod free volume, neglecting all the intermediate mechanisms occurring, e.g., long-distance axial transfer, percolation, grain-face diffusion, re-solution from grain-boundary bubbles (Pizzocri et al., 2020; Pastore et al., 2013; Bernard et al., 2002; Rest, 2003).

This behaviour is supported by experimental observations of fractured surfaces of UO_2 showing that the grain boundaries are populated by large, lenticular bubbles (White, 2004). If the grain-boundary bubble density is N_{gb} (bubbles m^{-2}) and the bubble average (projected on the grain boundary) area is A_{gb} (m^2), the fraction of the grain boundary covered with grain-boundary bubbles is $N_{gb}A_{gb}$, defined as fractional coverage F_c (/). The critical, or saturation, value of F_c that determines the interconnection of the grain boundary bubbles is set to $F_{c,sat} = 0.5$, in line with experimental observations (White, 2004; Veshchunov, 2008; White et al., 2006).

The intra-granular behaviour of radioactive FG is modelled as follows. Considering a spherical fuel grain, the diffusion of radioactive FG towards the grain boundary is described following Booth formulation (Booth, 1957), according to Eq. (1):

$$\frac{\partial C(r,t)}{\partial t} = D_{eff}(F,T)\nabla^2 C(r,t) - \lambda C(r,t) + S(F) \tag{1}$$

where F(fiss m^{-3} s^{-1}) is the fission rate density, T(K) is the (local) fuel temperature, t(s) is the time, r(m) is the radial position in the ideal spherical grain, λ (s^{-1}) is the decay rate and $S = yF$ (at m^{-3} s^{-1}) is the production rate of the gas, y (at fission^{-1}) is the cumulative fission yield. The concentration C (at m^{-3}) represents the residual amount of intra-granular FG. The effective diffusivity D_{eff} (m^2s^{-1}) includes a correction due to the first precursor through a factor α (/), as in the ANS 5.4–2010 methodology[1] (Turnbull and Beyer, 2010; Zullo et al., 2022b; Zullo et al., 2022c). Also, it includes the combined effect of trapping-in (Ham, 1958) and irradiation-induced re-solution (Speight, 1969) from

[1] The precursor enhancement factor α (/) is a corrective factor which takes into consideration the (observed) diffusivity increases for some radioactive gaseous and volatile FPs (Brown and Faircloth, 1976). As reported in the ANS 5.4–2010 methodology (Turnbull and Beyer, 2010), and based on the work of Friskney et al. (Friskney and Speight, 1976), for the first precursor we can write $\alpha = \left(\frac{1-\left(\frac{y_0}{x_0}\right)^3}{1-\left(\frac{y_0}{x_0}\right)^2}\right)^2$. In this expression, $y_0 = \sqrt{D_p/\lambda_p}$ and $x_0 = \sqrt{D_i/\lambda_i}$, where λ_p and λ_i are the decay rates of the precursor and consider isotope, respectively, and D_p and D_i are the diffusion coefficients of the precursor and considered isotope, respectively. Lastly, Section 2 deals only with xenon and krypton (gaseous fission products). In line with the state-of-the-art modelling of fission gas behaviour (Turnbull and Beyer, 2010; Zullo et al., 2022b; Zullo et al., 2022c), it is reasonable to assume their diffusivities equal.

intra-granular bubbles, according to the approach proposed by Speight (Speight, 1969), further extended by White and Tucker[2] (White and Tucker, 1983). The expression for the single-atom diffusivity $D(m^2/s)$ is the legacy expression from the work of Turnbull et al. (Turnbull et al., 1988), in line with the modelling adopted in SCIANTIX for the inert gas behaviour (Pizzocri et al., 2020; Turnbull et al., 1988), and the classical interpretation for the xenon mobility in irradiated UO_2 (Rest et al., 2019). In the end, g (s^{-1}) being the trapping rate and b (s^{-1}) the re-solution rate, respectively, the effective diffusivity is then given by $D_{\text{eff}} = \alpha \frac{b}{b+g} D$. The numerical solution of Eq. (1) is calculated via spectral diffusion algorithms, proved to be effective under constant and, most importantly, fast transient conditions[3] (Pastore et al., 2018; Pizzocri et al., 2016; Zullo et al., 2022a).

The inter-granular behaviour of short-lived fission gases is modelled following a physics-based approach valid for stable FG behaviour, which describes fission gas release and gaseous fuel swelling (Pizzocri et al., 2020; Pastore et al., 2013; White, 2004). This choice lies on the assumption that grain-boundary bubble growth, coalescence, and interconnection are mainly driven by stable FGs and that short-lived FGs, negligible in mass with respect to stable isotopes, are not relevant in determining the grain-boundary bubble evolution (Zullo et al., 2022b). In the end, grain-boundary bubble interconnection proceeds until grain-boundary saturation, and this process represents an incubation time for the onset of the thermal release (Vitanza et al., 1979). The incubation period is caused by the initially closed porosity of the fuel microstructure and for short-lived radioactive FGs, this delay is significant. Hence, suitable modelling of this incubation period is required. From the modelling point of view, the grain-boundary bubble behaviour is currently described according to works of White (White, 2004) and Pastore et al. (Pastore et al., 2013). In line with the modelling of stable FGs, the concentration of radioactive FGs accumulated at the grain boundary C_b (at m^{-3}) is given by:

$$\frac{dC_b}{dt} = -\left(\frac{3}{a} D_{eff} \frac{\partial C}{\partial r}\right)_{r=a} - \lambda C_b - R \tag{2}$$

The release rate R (at $m^{-3}\ s^{-1}$) accounts for the FG atoms accumulated at grain boundaries that are released to the fuel rod free volume as soon as the grain-boundary saturation occurs (Pizzocri et al., 2020; Pastore et al., 2013; Zullo et al., 2022b).

2.2. Fuel-to-gap model for the release of radioactive gas in TRANSURANUS-NINE

Fission product transport mechanisms inside and outside the fuel differ according to species (e.g., due to different chemical affinity) and among isotopes of the same species (e.g., due to radioactive decay). When the release outside the cladding is considered in defective fuel rods, the decay rate of different isotopes plays a relevant role by evaluating the coolant activity (White and Tucker, 1983; Pastore et al., 2013; White, 2004). For these reasons, thoroughly studying transport and concentration of different fission products in nuclear systems requires to evaluate each isotope separately.

At the current state of development, the TRANSURANUS code[4] considers many stable isotopes of Xe, Kr, Cs and Nd, and the following unstable isotopes: ^{133}Xe, ^{135}Xe, and ^{85}Kr. The code simulates the production of these isotopes through fission events, and by correcting the fission yields of the unstable isotopes with some empirical multiplication factors to account only for the equilibrium concentrations. Then, the production of each species is calculated as the sum of the production of all the isotopes of such species, e.g., the sum of ^{133}Xe, ^{135}Xe and the stable isotopes of xenon gives the final production of xenon. Doing this, the information referred to single isotopes is lost.

Besides, in TRANSURANUS, the release of gaseous and volatile radioactive (in particular, short-lived) fission products can be calculated by using the ANS-5.4 methodology (Turnbull and Beyer, 2010; Turnbull, 2001). This semi-empirical approach yields the release-to-birth ratio of some isotopes of xenon, krypton, and iodine, and when coupled with corresponding fission yields produces the released number of atoms.

To provide TRANSURANUS with a more robust option to assess the production and release of gaseous and volatile radioactive FPs, an alternative option has been implemented within the R2CA project at NINE, separating the contribution of each isotope of interest and extending the mechanistic modelling of stable fission gases to radioactive isotopes.[5] The following isotopes have been considered in the development:

- ^{128}Xe, ^{129}Xe, ^{130}Xe, ^{131}Xe, ^{132}Xe, ^{133}Xe, ^{134}Xe, ^{135}Xe, ^{136}Xe, ^{137}Xe, ^{138}Xe
- ^{80}Kr, ^{82}Kr, ^{83}Kr, ^{84}Kr, ^{85}Kr, ^{86}Kr, ^{87}Kr, ^{88}Kr, ^{89}Kr
- ^{133}Cs, ^{135}Cs, ^{137}Cs, ^{138}Cs
- ^{131}I, ^{132}I, ^{133}I, ^{134}I, ^{135}I, ^{136}I, ^{137}I, ^{138}I

The isotopes are interconnected by decay processes (β^-) and capture events (σ_c), as schematically shown in Fig. 1.

To compute the FP inventory in the fuel the following equation has been considered for each isotope:

$$\frac{d\,{}^{A}_{Z}N(t)}{dt} = y_f q - \lambda_{N^A_Z}\,{}^{A}_{Z}N(t) - \sigma_{c_{N^A_Z}}\,\Phi\,{}^{A}_{Z}N(t) \tag{3}$$

In Eq. (3), N is the local concentration (namely the production) of the FP isotope (Z, A) in the fuel $\left(\frac{\mu mol}{mm^3}\right)$, y_f is the fission yield $\left(\frac{\mu mol}{W}\right)$, q is the local power density $\left(\frac{W}{mm^3}\right)$, $\sigma_{c_{Z}^{A}N}$ is the neutron capture cross section evaluated at thermal energy (cm^2), and Φ is the thermal neutron flux $\left(\frac{n}{cm^2 s}\right)$. The fission yields, decay constants and neutron capture cross sections are evaluated from the JEFF-3.3 library (White and Tucker, 1983; Pastore et al., 2013; White, 2004). This approach to evaluate the isotopes inventories has been implemented in TRANSURANUS, and the use of cumulative fission yields has been assessed through a comparison with the Serpent code (White and Tucker, 1983; Pastore et al., 2013; White, 2004). The calculation of the release of radioactive isotopes is based on the mechanistic TRANSURANUS option to describe the stable (xenon and krypton) fission gas behaviour (White and Tucker, 1983; Pastore et al., 2013; White, 2004). Namely, stable FGs are produced inside the UO_2 grains, they migrate towards the grain boundaries predominantly via thermal or irradiation-induced diffusion and accumulate in grain-

[2] In the SCIANTIX code, the model for intra-granular FG behaviour is tightly bound to the mechanistic description of the intra-granular bubble (average) size and concentration, for which we refer to the work of Pizzocri et al. (Pizzocri et al., 2018) for a more detailed description. Concerning the intra-granular FG diffusion, the diffusivity is influenced by the irradiation-induced re-solution from and trapping in intra-granular bubbles, assumed immobile (Eq. (2)). The trapping rate g (s^{-1}) is calculated as $g = 4\pi D R_{ig} N_{ig}$ (White and Tucker, 1983; Ham, 1958), with R_{ig} (m) and N_{ig} (bub m^{-3}) average intra-granular bubble radius and density, respectively, and it represents the rate of FG atoms trapping into bubbles. The re-solution rate b (s^{-1}) is assumed to be mainly heterogeneous (i.e., irradiation-induced (White and Tucker, 1983; Lösönen, 2000; Turnbull, 1971; Govers et al., 2012), and written as $b = 2\pi\mu_{ff}(R_{ig} + R_{ff})^2 F$, where μ_{ff}(m) is the average length of a fission spike and R_{ff} (m) its average influence radius.

[3] The latter feature demonstrated to be essential when considering short-lived isotopes, in which the time constants of Eq. (1) may be dominated by high value of λ, competitive with diffusion rates D/a^2. This topic has been explored in depth in Zullo et al. (2022a).

[4] In this work, the reference TRANSURANUS version is the v1m6j21.

[5] In the current work, chemical interactions between non-inert FPs are neglected and will be object of further developments involving thermo-chemical libraries.

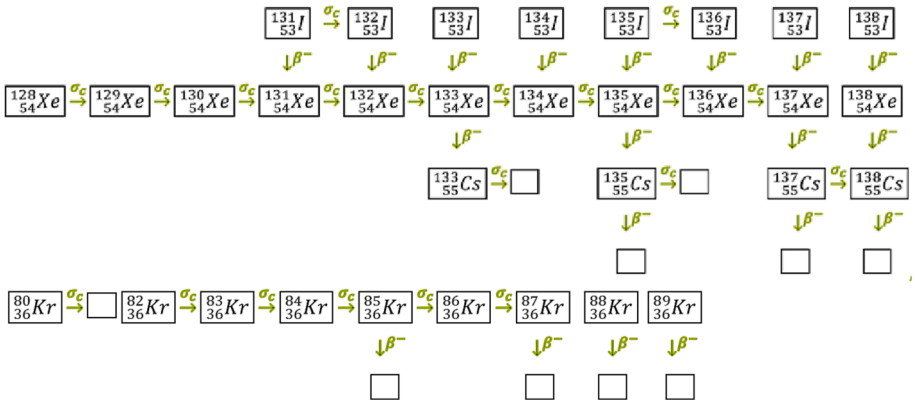

Fig. 1. Relationship among radioactive decays and capture events for the list of isotopes considered by the development of the new model implemented in TRANSURANUS (white boxes represent isotopes not considered in the model described, e.g., barium and rubidium).

boundaries bubbles. The intra-granular diffusion of stable fission gas in TRANSURANUS is governed by:

$$\frac{\partial C(r,t)}{\partial t} = D_{eff}(F,T)\nabla^2 C(r,t) + S(F) \tag{4}$$

The intra-granular diffusivity D_{eff} can be chosen among different options. Notwithstanding, none of them considers the possibility to diffuse in a hyper-stoichiometric fuel matrix. The hyper-stoichiometric condition may occur in presence of a cladding defect. Indeed, in a defective rod the coolant may enter the fuel-cladding gap permitting oxidation of both the fuel and the cladding. It is known that in oxidizing conditions the release of the fission products increases due to changes in the intra-granular diffusivity (Massih, 2018; Dobrov et al.; Higgs et al., 2007; Olander, 1998, 2017; Killeen and Turnbull), hence it is of interest to account for this process from a mechanistic point of view. In the work carried out by Killeen and Turnbull (Killeen and Turnbull), there are reported a series of experiments in which the release of ^{85}Kr from hyper-stoichiometric uranium dioxide was measured under annealing conditions, in CO/CO_2 atmospheres (White and Tucker, 1983; Pastore et al., 2013; White, 2004) and an expression for the intra-granular diffusivity is given. Nevertheless, the equation is somewhat inconvenient for a fuel rod modelling code due to its complexity and the presence of many empirical constants and parameters, which may vary depending on the isotope and atmosphere considered. For this reason, Kim (Kim, 2000) provides a simplified practical expression for the intra-granular diffusivity of fission gas in UO_{2+x}. In Kim's formulation the intrinsic thermal contribution D_1 (m^2/s) is corrected with a factor that accounts for the observed enhanced diffusivity under hyper-stoichiometric conditions, resulting in:

$$D_1 = 7.6 \times 10^{-10} e^{-\frac{35000}{T}} f(x) \tag{5}$$

$$f(x) = 1 + 493x + 32182x^2 \tag{6}$$

The variable x (/) indicates the deviation from stoichiometry. Eqs. (5) and (6) are considered valid in the hyper-stoichiometry range $0.005 \leq x \leq 0.12$, and in the temperature range 1000 K $\leq T \leq$ 1600 K. The coefficient D_1 together with the thermal irradiation enhanced and the a-thermal components contributes to the calculation of the single-atom diffusivity defined from Turnbull et al. (Turnbull et al., 1988). Then, the intra-granular diffusivity implemented in TRANSURANUS is defined according to the approach proposed by Speight (Speight, 1969), further extended by Van Uffelen (Van Uffelen et al., 2011):

$$D_{eff} = \frac{b}{b+g} D_s + \frac{g}{b+g} D_b \tag{7}$$

That considers trapping (g) and irradiation-induced resolution rates (b). The effective diffusion coefficient D_{eff} is decomposed in two components: the first one considering only the fraction of FPs not trapped in intra-granular bubbles (i.e., available as single-atoms in solution in the fuel matrix, with diffusion coefficient D_s) and the second one referring to the population of FPs trapped into bubbles and available to diffuse only through bubble mobility[6] D_b.

As previously stated, in this work the mechanistic description of stable fission gas diffusion, available in TRANSURANUS, has been extended to gaseous and volatile radioactive fission products. Eq. (4) can be solved by both URGAS and FORMAS algorithms (Lassmann and Benk, 2000; Forsberg and Massih, 1985; Forsberg and Massih, 1985) that are tailored for the diffusion equation without the decay loss, hance it has been approximated as valid to describe the diffusion of short-lived fission products. In the current implementation, the stoichiometry deviation x equals the radially averaged oxygen-to-metal ratio in each section (or slice) of the discretized fuel rod. Further developments of this description will consider the development of a dedicated solver for Eq. (1) in TRANSURANUS as well, and the formulation of an oxygen redistribution model inside the fuel matrix (including local stoichiometry variations) and the analysis of the thermal effect on the hyper-stoichiometry conditions. Lastly, grain-boundary processes (e.g., grain-boundary bubble evolution, onset for fission gas release and gaseous fuel swelling) are determined by the evolution of stable fission gases, according to (Pastore et al., 2013).

2.3. Benchmark of fuel-to-gap models for the release of radioactive gas against the CONTACT1 irradiation test

The two versions of the TRANSURANUS code previously described (i.e., TRANSURANUS coupled with SCIANTIX and TRANSURANUS extended by NINE) have been used to reproduce the CONTACT1 irradiation experiment, from the IFPE open database (Bruet et al., 1980; Charles et al., 1983), to assess and benchmark their predictive capabilities when calculating the release of short-lived gaseous and volatile FPs. Along with these two TRANSURANUS versions, the comparison includes the prediction of TRANSURANUS when using the semi-empirical ANS

[6] The intra-granular bubble mobility, appearing in Eq. (12) through the effective diffusivity D_b, has been investigated in several works (Van Uffelen et al., 2011; Evans, 1994; Verma et al., 2020; Verma et al., 2019; Moal et al., 2014; Veshchunov and Tarasov, 2013). Its use was exploited to investigate the large fission gas release at high temperatures (above 1600°C) in annealing conditions and during transients, while it provides a negligible contribution to the fission gas release in normal PWR conditions (Van Uffelen et al., 2011). For this reason, the intra-granular bubble mobility is not included in Eq. (2) and does not determine a difference in the fission gas release during the CRUSIFON experiments shown in Section 3.

5.4–2010 (Turnbull and Beyer, 2010), recently implemented in the code in the frame of the R2CA European project (R2CA, 2019). In Fig. 2 we show the CONTACT1 linear heat rate provided as input to TRANSURANUS, as a function of the burn-up. The purpose of the CONTACT1 irradiation experiment was to improve the general understanding of the fuel rod performance and the release of short-lived FG isotopes (Bruet et al., 1980; Charles et al., 1983). Available data from IFPE documentation, shown in Fig. 3, include release-to-birth ratios (R/B) of ^{133}Xe, ^{135}Xe, ^{137}Xe, ^{138}Xe, ^{87}Kr, ^{88}Kr and ^{89}Kr as a function of the burn-up. The monitored isotopes being inert gases (or, in other words, neglecting chemical interactions) are treated in the same way by the considered codes, in terms of the transport processes from inside the fuel to the rod free volume. For this reason, in Fig. 4 we compare the R/B of one isotope, the short-lived ^{133}Xe isotope.

In Fig. 4, we show the ^{133}Xe R/B, as calculated by TRANSURANUS and the ANS 5.4–2010 methodology, TRANSURANUS-NINE and TRANSURANUS//SCIANTIX. When TRANSURANUS adopts the semi-empirical ANS 5.4–2010 methodology (Turnbull and Beyer, 2010) to predict ^{133}Xe R/B (green line in Fig. 4), the calculation underestimates the data (black dots in Fig. 4), hence the gap activity as well. This underprediction has revealed to be systematic in the simulation of this case (Zullo et al., 2022b; Zullo et al., 2022c), and it can be attributed to the calibration behind the semi-empirical nature of the ANS 5.4–2010 methodology, that is trained on a different experimental database (Turnbull and Beyer, 2010; Turnbull, 2001). In addition, the release dynamic is not well represented since the methodology essentially follows the input linear heat rate (Fig. 2). This constitutes a crucial limitation when considering fast transient scenarios and their dynamics (such as in the case of a fuel failure event) potentially resulting in the unreliability of the ANS 5.4–2010 methodology, that can be overcome with the help of TRANSURANUS//SCIANTIX or TRANSURANUS-NINE.

Detailing the performance of the TRANSURANUS code extended by NINE, as described in Section 2.2, for the CONTACT1 simulation, Eq. (4) is solved with the URGAS algorithm (Elton and Lassmann, 1987) (including Eq. (6) with $x = 0$ in absence of oxidating environment). The resulting flux of atoms from the intra-granular region is then combined with the TRANSURANUS mechanistic inter-granular gas modelling (Pastore et al., 2013; Van Uffelen et al., 2011) and the inventory calculation (Eq. (3)) to estimate the release-to-birth ratio of short-lived FG isotopes. The predicted R/B curve in Fig. 4 (i.e., the blue line) follows a behaviour qualitatively like that described for the previous case (TRANSURANUS//SCIANTIX). Namely, it is noticeable the R/B increase with burn-up during the irradiation. Indeed, CONTACT experiments confirm the difference of the release mechanisms at low and high temperature, being 1000 °C the transition temperature. When the fuel temperature overcomes the transition temperature, there is a strong increase in the release, which is clearly visible in the experimental data, and it is correctly predicted by the computer codes as well. Furthermore, the range of burn-up investigated reveals its influence on the release at such high linear heat rate irradiation conditions, and in line with such experimental evidence the computer codes calculate increasing release even below the transition temperature. Such influence from the fuel burn-up is typical of high rating conditions, and it is not visible for fuels working in the irradiation conditions of power reactors, e.g., at an average linear heat rate of about 25 kW m^{-1}. Concerning TRANSURANUS coupled with the mechanistic code SCIANTIX (Section 2.1), the modelling includes the fundamental intra-granular production-diffusion-decay processes, and inter-granular accumulation-decay-release processes (Zullo et al., 2022b; Zullo et al., 2022c; Zullo et al., 2022a). Because of the SCIANTIX modelling, the predicted R/B (red line in Fig. 4) increases during the irradiation (i.e., with increasing burn-up), towards an equilibrium value. The overestimation of the measured release (black dots in Fig. 4) is mainly attributed to the current SCIANTIX modelling of grain-boundary bubble microcracking, a mechanism that is initiated by sudden variations in temperature (in this CONTACT1 case, in correspondence with linear heat rate variations) and has been shown to contribute to this overestimation (Zullo et al., 2022c).

3. Release of gaseous and volatile radioactive fission products in the primary coolant under stationary operation

The present section outlines a development that has been included in the TRANSURANUS version extended by NINE, towards the prediction of radioactive release from defective fuel rods, and, ultimately, the estimation of the fission product isotopes concentrations in the primary coolant. The model that is descried in this section (gap-to-coolant release) is an extension of the previous fuel-to-gap release model (Section 2.2) operated in the TRANSURANUS-NINE version, within the

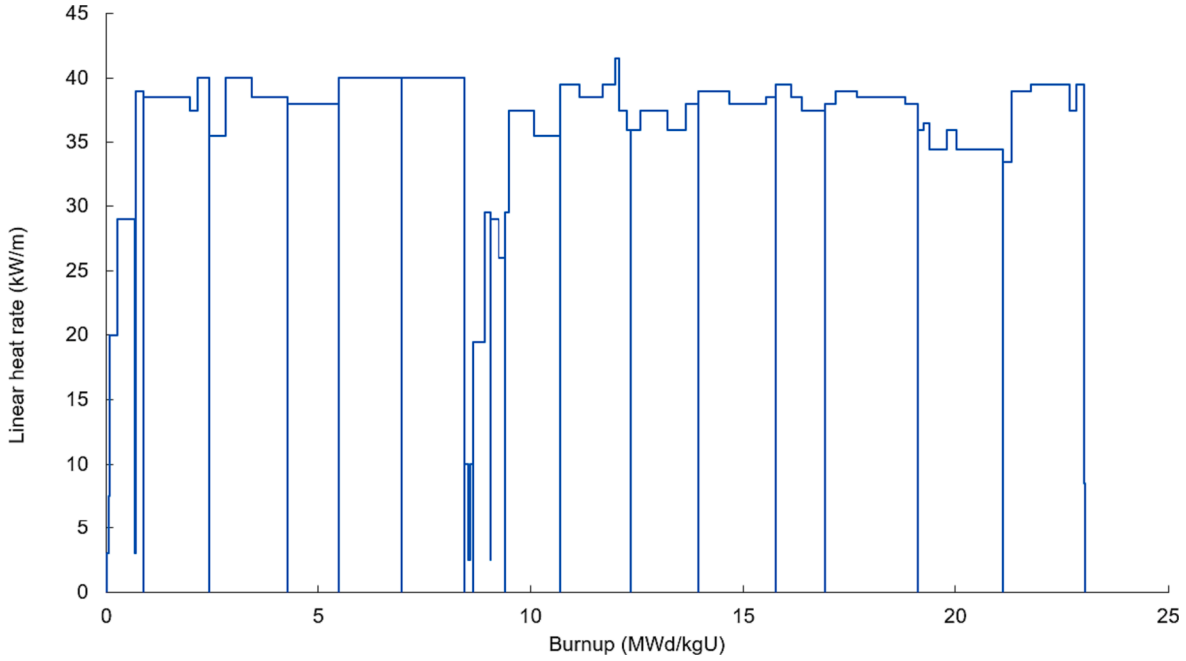

Fig. 2. Input linear heat rate for the simulation of CONTACT1 irradiation experiment in TRANSURANUS, as a function of the burn-up.

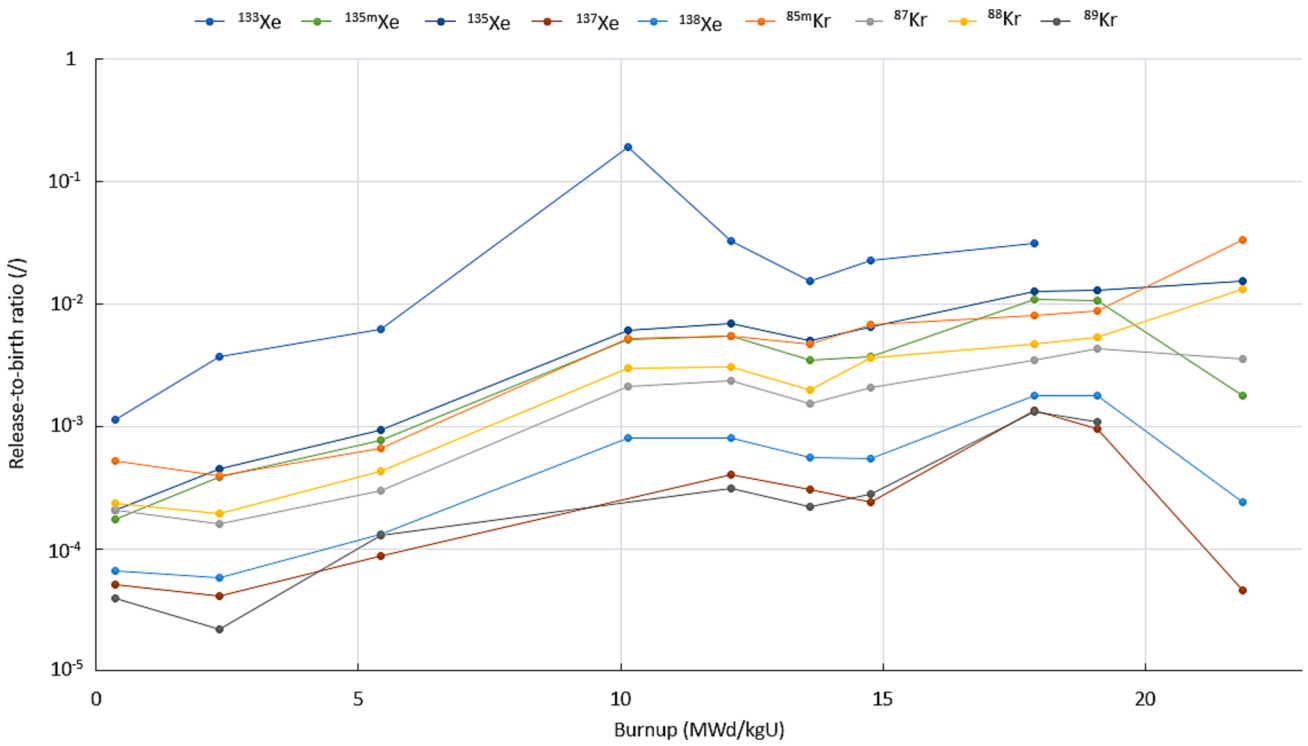

Fig. 3. Measured release-to-birth ratios of short-lived fission gases, monitored during the CONTACT1 irradiation experiment, as a function of the burn-up (Bruet et al., 1980; Charles et al., 1983; Zullo et al., 2022b). The dots are connected for sake of readability.

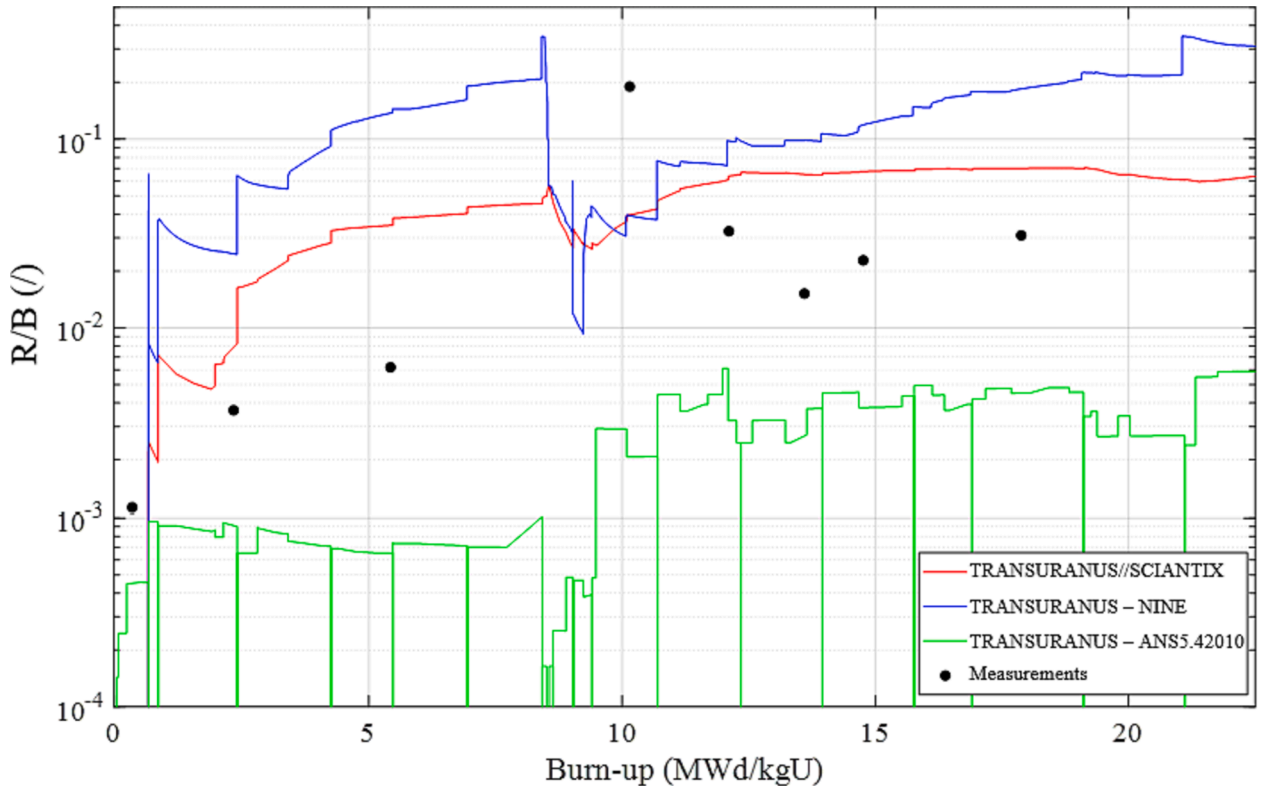

Fig. 4. Release-to-birth ratio of ^{133}Xe isotope, measured during the CONTACT1 experiment (data reported as black dots) along with code calculation results. The green line represents the prediction from ANS 5.4–2010 methodology, the semi-empirical algorithm recently implemented in TRANSURANUS (Turnbull and Beyer, 2010; Zullo et al., 2022c). The red line represents the calculation from the TRANSURANUS//SCIANTIX version (Zullo et al., 2022b; Zullo et al., 2022c). The blue line represents the calculation from the mechanistic TRANSURANUS fission gas behaviour model, extended at NINE to the radioactive isotopes as described in Section 2.2.

R2CA European project (R2CA, 2019). The model is based on a simplified approach, which is detailed in Section 3.1. It is applicable only in steady state conditions that allow to reach an equilibrium between the release from the fuel and the release out of the defect. Under this hypothesis there is no axial transport and accumulation of fission gas isotopes in the gap, which allows to neglect the chemical interactions on fission products. Section 3.2 presents the results of the application of the model to simulate the CRUSIFON1bis and CRUSIFON2 tests. Section 3.3 is dedicated to the final discussion and future development perspectives.

3.1. Evaluation of isotopes escape rate coefficients and coolant concentrations

The gap-to-coolant model chosen as a starting point for the analysis of defective fuel rods, which was also the most in line with a direct implementation in TRANSURANUS, is the generalized Lewis model (Lewis, 1990), echoed in the recent work of Veshchunov (Veshchunov, 2019). The model is based on a phenomenological first-order kinetic model. The gap-to-coolant transport of gaseous and volatile FPs through the cladding defect is hence described as a first-order rate process:

$$\frac{dn_i}{dt} = q_i - R_i - \lambda_i n_i \tag{8}$$

where $n_i\left(\frac{\text{at}}{\text{m}^3}\right)$ is the mean concentration of the i-th isotope in the fuel rod free volume (i.e., including the volumes of fuel-cladding gap and fuel rod plenum), $q_i\left(\frac{\text{at}}{\text{m}^3\text{s}}\right)$ is the release rate of the i-th isotope from the fuel (per unit volume of the fuel rod free volume), and $R_i\left(\frac{\text{at}}{\text{m}^3\text{s}}\right)$ is the release rate from the gap into the coolant. R_i is assumed to be proportional to n_i through a phenomenological escape rate coefficient $\varepsilon\left(\frac{1}{\text{s}}\right)$:

$$R_i = \varepsilon n_i \tag{9}$$

If an equilibrium between the fuel-to-gap release and the gap-to-coolant release is reached, the following relation can be used to estimate the escape rate:

$$q_i = R_i = \varepsilon n_i \text{ hence } \varepsilon = \frac{q_i}{n_i} \tag{10}$$

In the present discussion, axial transport phenomena are neglected, and the focus is on PWR conditions, for which a weak dependence of ε on the defect size can be considered as valid (Veshchunov, 2019).

Evaluating the ε phenomenological defective cladding escape rate coefficients is the crucial point to estimate the primary coolant activity in the event of fuel failure (Veshchunov, 2019). Escape rate coefficients are calculated using Eq. (10).

3.2. Integral irradiation experiment results

There is a small number of experimental data available in open literature about the coolant activity due to radioactive gaseous and volatile FPs released from a defective fuel rod. To the best of the authors knowledge, the IFPE open database includes data from the CRUSIFON program (Harrer et al., 1980; Harrer et al., 1981), representative of irradiation experiments in which a cladding failure was mechanically imposed.

Therefore, in this section we show the results of the calculated fuel-to-gap release rate coefficients and isotopes coolant concentrations of the CRUSIFON1bis and CRUSIFON2 tests.

The aforementioned tests are part of a series of loop experiments performed on short fuel rods by CEA in France with the aim to measure and interpret the release rate from defective rods of fission gases and iodine, under steady state and transient power operating conditions. Both the tests were performed in the Siloe reactor in the Bouffon loop, which consisted of two vertical tubes connected at both ends to form a continuous circuit for pressurised water. The experimental fuel rod was situated in the bottom of one tube below a heater, which provided an up current of cooling water over the experimental fuel rod. After some cycles at almost constant power, a cladding defect that consisted of a small crack was forcibly opened in a precise time instant, during both experiments. From that point on the coolant activity began to be recorded. The observed fission product release was made up of bursts followed by a constant low-level release.

Fig. 5 shows the escape rate coefficients calculated by means of Eq. (10), after the defect opening; in particular, two isotopes (i.e., ^{138}Xe and ^{87}Kr) evaluated during the CRUSIFON1bis experiment are reported as an example. Their behaviour is representative of almost all the isotopes evaluated considering both experiments. The stationary operating conditions at which it make sense to apply the model are indicated by the vertical blue lines. We can assume to be in the stationary condition of equal releases from and out of the gap, considering the constant linear heat rate and especially the stationary coolant activity measured during the experiment (Harrer et al., 1980; Harrer et al., 1981). In the neighbourhood of such instants (the same approach was used for the Crusifon2 test) we evaluated the average escape rate coefficients, considering a range between maximum and minimum values, all reported in Table 1 including the decay rates. Such average escape rate coefficients are adopted in the TRANSURANUS-NINE version to evaluate the isotopes coolant concentrations, as previously described. Results are reported in Fig. 6, considering the same isotopes and test of Fig. 5. Along with the calculations, tabulated data from IFPE documentation (Harrer et al., 1980; Harrer et al., 1981) are reported in Fig. 6. The green dots represent tabulated data of nuclide measurement obtained by sampling and spectrometry of water samples, while the green line represent coolant concentration that has been interpolated according to the measured global activity of the coolant in the experimental setup. The prediction of this version of TRANSURANUS extended by NINE (blue dots in Fig. 6, inside the band of variation of calculated data) gives a qualitative insight on the coolant concentration in stationary conditions, namely the ones assumed in the previous section for the phenomenological rate theory model.

3.3. Discussion

The escape rates span a wide range of values among different isotopes (from about 10^{-6} to 10^{-3} s^{-1}). Some considerations should be kept in mind when considering those results. First, the model is based on releases balance assumption and a simplified first order kinetic theory. Therefore, we are neglecting some important phenomena, like the gap composition evolution and the bursts during the power transients. In addition, the uncertainties associated with the measurements are not known. All these elements contribute to the final release from defective fuel and their importance should be further investigated in more detailed and specific analyses to be assessed.

Moreover, not all the isotopes are reported in Table 1 since higher escape rates are obtained for some iodine isotopes and the caesium ones according to this evaluation. This should not mean that iodine and caesium are released more than others, and a further analysis should be also envisaged to investigate the smaller spread of the resulting escape rates (i.e., min. and max. values have almost the same order of magnitude). The data show that the behaviour of the iodine isotopes is distinct from that of the gases through their capacity to be trapped on internal surfaces of the rod. A possible reason that justifies the scarce representativeness of the iodine results is that a smaller quantity remained to be released during the steady-state conditions after spiking phenomena, due to coolant entering and washing out the gap.

In particular, on reactor startup the fuel expands with heat up, the water turns to steam in the gap and noble gases are convectively forced out of the rod. On reactor shutdown, noble gases may be trapped in the plenum in the vertical rod (depending on the defect location) and thereby prevented from escaping. Nevertheless, the iodine escape rate coefficient increases due to Nernst diffusion as the water-filled gap dissolves the Cs-I deposits with a more rapid ionic diffusion in the water

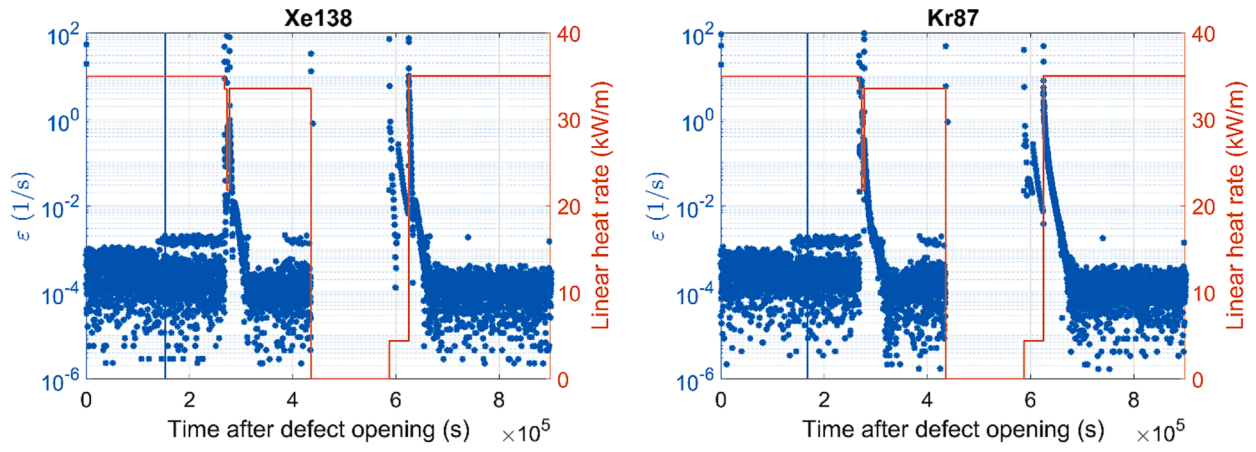

Fig. 5. Escape rate coefficients from defective cladding to primary coolant of ^{138}Xe and ^{87}Kr, after defect opening in the CRUSIFON1bis experiment (blue dots). The right y-axis reports the linear heat rate (red line). The vertical blue line at about 1.7x10^5 s represents the time at which the steady-state condition is reached, from which stationary coolant concentrations were measured.

Table 1
Fission products isotopes decay rates and escape rate coefficients evaluated during stationary operation of CRUSIFON1bis and CRUSIFON2 irradiation experiments.

Isotope	λ (1/s)	ε (1/s) CRUSIFON1bis		CRUSIFON2		average
		min	max	min	max	
^{128}Xe	–	2.28x10^{-6}	1.43x10^{-5}	1.71x10^{-6}	1.03x10^{-5}	5.62x10^{-6}
^{129}Xe	–	2.15x10^{-6}	1.61x10^{-5}	1.61x10^{-6}	2.09x10^{-5}	7.22x10^{-6}
^{130}Xe	–	1.67x10^{-6}	1.67x10^{-5}	2.50x10^{-6}	1.51x10^{-5}	6.76x10^{-6}
^{131}Xe	–	7.48x10^{-6}	1.25x10^{-5}	1.87x10^{-6}	1.50x10^{-5}	7.91x10^{-6}
^{132}Xe	–	6.85x10^{-6}	1.14x10^{-5}	1.72x10^{-6}	1.38x10^{-5}	7.25x10^{-6}
^{133}Xe	1.52x10^{-6}	2.25x10^{-6}	1.42x10^{-4}	1.94x10^{-6}	6.34x10^{-5}	2.48x10^{-5}
^{134}Xe	–	8.86x10^{-6}	1.33x10^{-5}	2.68x10^{-6}	1.34x10^{-5}	8.62x10^{-6}
^{135}Xe	2.09x10^{-5}	1.33x10^{-5}	1.94x10^{-3}	4.03x10^{-6}	2.14x10^{-4}	1.68x10^{-4}
^{136}Xe	–	3.96x10^{-6}	7.44x10^{-6}	1.50x10^{-6}	1.80x10^{-5}	6.06x10^{-6}
^{137}Xe	3.03x10^{-3}	6.82x10^{-6}	2.05x10^{-3}	1.02x10^{-5}	9.20x10^{-4}	2.73x10^{-4}
^{138}Xe	8.20x10^{-4}	1.16x10^{-5}	2.04x10^{-3}	1.97x10^{-5}	9.16x10^{-4}	3.06x10^{-4}
^{80}Kr	–	2.05x10^{-6}	7.70x10^{-6}	1.68x10^{-6}	2.52x10^{-5}	6.22x10^{-6}
^{82}Kr	–	4.51x10^{-6}	8.45x10^{-6}	1.72x10^{-6}	1.90x10^{-5}	6.72x10^{-6}
^{83}Kr	–	4.72x10^{-6}	1.48x10^{-5}	1.76x10^{-6}	1.76x10^{-5}	7.81x10^{-6}
^{84}Kr	–	4.78x10^{-6}	1.27x10^{-5}	1.92x10^{-6}	2.49x10^{-5}	8.53x10^{-6}
^{85}Kr	–	5.96x10^{-6}	1.79x10^{-5}	1.64x10^{-6}	1.31x10^{-5}	7.89x10^{-6}
^{86}Kr	–	1.29x10^{-6}	9.70x10^{-6}	1.94x10^{-6}	9.72x10^{-6}	4.49x10^{-6}
^{87}Kr	1.51x10^{-4}	2.18x10^{-5}	1.94x10^{-3}	2.43x10^{-6}	9.76x10^{-4}	2.74x10^{-4}
^{88}Kr	6.78x10^{-5}	6.05x10^{-6}	1.92x10^{-3}	1.77x10^{-4}	1.60x10^{-3}	4.72x10^{-4}
^{89}Kr	3.67x10^{-3}	2.10x10^{-5}	2.03x10^{-3}	8.57x10^{-6}	8.89x10^{-4}	2.97x10^{-4}

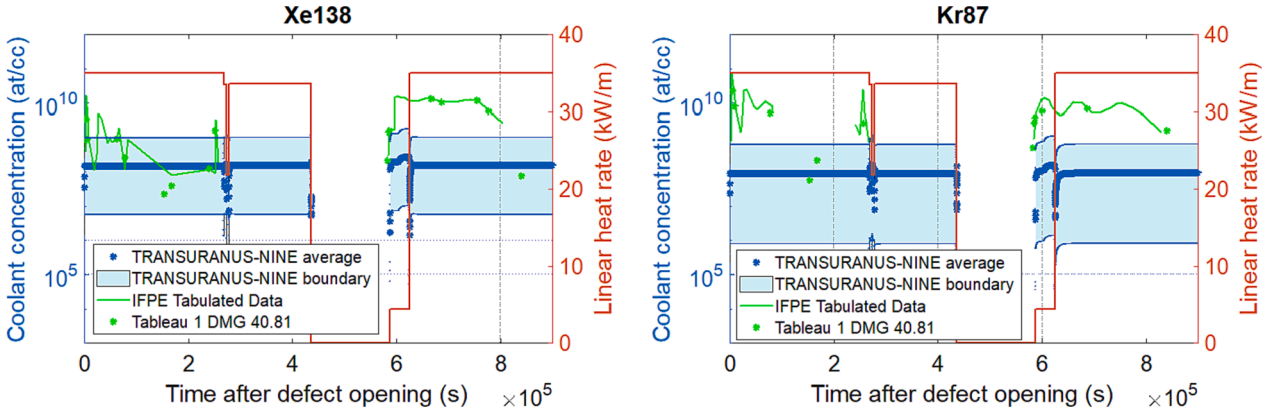

Fig. 6. Concentration of ^{138}Xe and ^{87}Kr in the coolant, after defect opening in the CRUSIFON1bis experiment. The blue dots represent the concentrations calculated with TRANSURANUS extended by NINE, inside the band of variation of calculated data (boundary). The green line represents the data reported in the IFPE documentation, interpolated from global activity measurements and the green dots represent experimental data from online measurements tabulated in the IFPE experimental report (i.e., Tableau DMG 40/81 (Harrer et al., 1980; Harrer et al., 1981)).

to the defect site (compared to Chapman-Enskog diffusion theory for the gaseous steam environment), depending on the presence of water or steam and adsorption/dissolution processes (Lewis et al., 2017). The resulting burst release phenomena should significantly change the fuel cumulative release provided by Eq. (10) that is used to calculate the gap escape rate under the hypotheses mentioned there, and thus compromise the meaning of the results presented in this work.

A similar transient burst release effect can be also observed for Xe and Kr, as reported by the green line and dots of Fig. 6, but the effect is smaller due to the lower chemical interaction of the noble gases. Indeed, a posteriori comparison with concentrations measured in the coolant (see Fig. 6) shows that measured data fall inside a band of variation of calculated data which consists of few orders of magnitude.

Finally, we managed to simplify and describe with a law based on releases equilibrium a phenomenon that is quite more complicated and intrinsically related to transient conditions. Indeed, the condition of the gap after the defect opening is the dominant process in modelling a defective rod and obtaining the final release rate to the coolant. It involves phase changes of water, FP stationary release and spiking release phenomena. Moreover, also the modified release from the fuel due to changes in the physical properties of the UO_2 resulting from contact with water or steam should have important feedbacks. These conditions largely determine any release due to recoil in the water, the kinetics of fission product transport within the gap, the degree of radiolysis occurring and the chemisorption/desorption of iodine isotopes; they can have a strong influence on the temperature and gas atom diffusivity of the fuel and thus the number of gas atoms available to the gap. It is an intrinsic transient mechanism that can be accurately modelled by the coupling of the fuel performance analysis (that can calculate fission gas production and release from the fuel, temperature distribution and oxidation in the fuel and cladding) with a proper description of the gap thermal–hydraulic dynamics (i.e., water evaporation and steam condensation, partial pressures evolution and non-condensable gas release into the coolant), which is the target of specific thermal-hydraulics code such as RELAP5-3D. This would be an interesting application moving towards a complete phenomenological first-order kinetic model, as in Refs. (Veshchunov, 2019; Lewis, 1990); for future improvements of fast-running FPCs (as TRANSURANUS) when evaluating the radiological consequences of accidental scenarios, e.g., in fuel rod failure events.

4. Conclusions

This paper presents the results of a collaborative activity of benchmark and assessment towards modelling the release of radioactive gaseous and volatile FPs from defective fuel rods, with a two-step approach (fuel-to-gap and gap-to-coolant release) not available in the state-of-the-art TRANSURANUS fuel performance code. Due to the complexity of the phenomenon, we compare the outcomes of different models implemented in or coupled to TRANSURANUS. The focus is on short-lived gases and volatile fission products that are of great interest when evaluating the radiological consequences of severe accidents with conventional fuel performance codes.

First, the fuel-to-gap radioactive release is benchmarked and assessed against the CONTACT1 irradiation experiment, from the IFPE experimental database. The gap activity, due to radioactive release, is calculated with the TRANSURANUS code, using the state-of-the-art methodology ANS 5.4–2010, and compared with the TRANSURANUS version coupled with SCIANTIX, and the TRANSURANUS version extended by NINE, with dedicated subroutines. Release-to-birth ratios calculated with TRANSURANUS//SCIANTIX and TRANSURANUS-NINE point out the predictive capability of the mechanistic approaches in reproducing a physically grounded release dynamic. On the other side, the semi-empirical ANS 5.4.-2010 methodology follows the input linear heat rate, this being a limitation when considering time-dependent scenarios (such as in the case of a fuel failure event). Future work will explore different stoichiometry-dependent diffusivities based on available correlations (Lewis, Jun. 2007) as well atomistic calculations (Andersson, 2014).

The TRANSURANUS-NINE code version has also been extended to model the gap-to-coolant release from defective fuel rods. The selected approach is based on the implementation of a phenomenological rate theory model, available in open literature. Moreover, two experiments from the IFPE open database (CRUSIFON1bis and CRUSIFON2) were considered to compare the calculated results of escaped isotopes coolant concentrations. Average values obtained for the escape rate coefficients are in agreement with other evaluations available in open literature, and the corresponding coolant concentrations manage to bound well the experimental data. Some further analyses should be performed to assess the behaviour of some particular fission product species like iodine and caesium, which may need a dedicated chemical study.

Lastly, further developments of the present work include a development of a grain-scale description of the fuel matrix oxidation in the SCIANTIX code and the extension of the TRANSURANUS formulation of an oxygen redistribution model inside the fuel matrix (with local stoichiometry variations) including the analysis of the thermal effects under hyper-stoichiometry conditions (via the impact on fuel material properties).

5. Disclaimer

Views and opinions expressed in this paper reflect only the authors' view and the European Commission is not responsible for any use that may be made of the information it contains.

CRediT authorship contribution statement

L. Giaccardi: Software, Investigation, Validation, Data curation, Visualization, Writing – original draft, Writing – review & editing. **M. Cherubini:** Conceptualization, Supervision, Visualization, Writing – review & editing. **G. Zullo:** Software, Investigation, Validation, Data curation, Visualization, Writing – original draft, Writing – review & editing. **D. Pizzocri:** Supervision, Methodology, Validation, Visualization, Writing – review & editing. **A. Magni:** Supervision, Methodology, Validation, Visualization, Writing – review & editing. **L. Luzzi:** Resources, Supervision, Funding acquisition, Project administration, Visualization, Writing – review & editing.

Declaration of Competing Interest

The authors declare that they have no known competing financial interests or personal relationships that could have appeared to influence the work reported in this paper.

Data availability

Data will be made available on request.

Acknowledgements

This project has received funding from the Euratom research and training programme 2014-2018 under grant agreement No 847656 (R2CA project).

References

Andersson, D.A., et al., 2014. Atomistic modeling of intrinsic and radiation-enhanced fission gas (Xe) diffusion in UO_{2+x}: Implications for nuclear fuel performance

modeling. J. Nucl. Mater. 451 (1–3), 225–242. https://doi.org/10.1016/j.jnucmat.2014.03.041.
Bernard, L.C., Jacoud, J.L., Vesco, P., 2002. An efficient model for the analysis of fission gas release. J. Nucl. Mater. 302 (2–3), 125–134. https://doi.org/10.1016/S0022-3115(02)00793-6.
Booth, A.H., 1957. A method of calculating fission gas diffusion from UO_2 fuel and its application to the X-2-f loop test. Atomic Energy of Canada Limited.
Brown, P.E., Faircloth, R.L., 1976. Metal fission product behaviour in high temperature reactors - UO_2 coated particle fuel. J. Nucl. Mater. 59 (1), 29–41. https://doi.org/10.1016/0022-3115(76)90005-2.
Bruet, M., Dodelier, J., Melin, P., Pointund, M.-L., 1980. CONTACT 1 and 2 experiments: Behaviour of PWR fuel rod up to 15000 MWd/tU. In: In IAEA Specialists' Meetting on Water Reactor Fuel Element Perfomance Computer Modelling, pp. 235–244.
Charles, M., Abassin, J.J., Baron, D., Bruet, M., Melin, P., 1983. Utilization of contact experiments to improve the fission gas release knowledge in PWR fuel rods. In: IAEA Specialists Meetiing on Fuel Element Performance Computer Modelling. Preston, pp. 1–18.
Dobrov, B.V., Likhanskii, V.V., Ozrin, V.D., Solodov, A.A., Kissane, M.P., Manenc, H., May 1998. Kinetics of UO_2 oxidation in steam atmosphere. J. Nucl. Mater. 255 (1), 59–66. https://doi.org/10.1016/S0022-3115(97)00364-4.
Dong, B., Li, L., Li, C., Zhou, W., Yin, J., Wang, D., 2019. Review on models to evaluate coolant activity under fuel defect condition in PWR. Ann. Nucl. Energy 124, 223–233. https://doi.org/10.1016/j.anucene.2018.10.009.
Elton, P.T., Lassmann, K., 1987. Calculational methods for diffusional gas release. Nucl. Eng. Des. 101 (3), 259–265. https://doi.org/10.1016/0029-5493(87)90054-9.
Evans, J.H., 1994. Bubble diffusion to grain boundaries in UO_2 and metals during annealing: a new approach. J. Nucl. Mater. 210 (1–2), 21–29. https://doi.org/10.1016/0022-3115(94)90218-6.
Forsberg, K., Massih, A.R., 1985. Diffusion theory of fission gas migration in irradiated nuclear fuel UO_2. J. Nucl. Mater. 135 (2–3), pp. https://doi.org/10.1016/0022-3115(85)90071-6.
Forsberg, K., Massih, A.R., 1985. Fission gas release under time-varying conditions. J. Nucl. Mater. 127 (2–3), pp. https://doi.org/10.1016/0022-3115(85)90348-4.
Friskney, C.A., Speight, M.V., 1976. A calculation on the in-pile diffusional release of fission products forming a general decay chain. J. Nucl. Mater. 62, 89–94.
JRC Karlsruhe (Germany). https://joint-research-centre.ec.europa.eu/jrc-sites-across-europe/jrc-karlsruhe-germany_en.
Govers, K., Bishop, C.L., Parfitt, D.C., Lemehov, S.E., Verwerft, M., Grimes, R.W., 2012. Molecular dynamics study of Xe bubble re-solution in UO_2. J. Nucl. Mater. 420 (1–3), 282–290. https://doi.org/10.1016/J.JNUCMAT.2011.10.010.
Ham, F.S., 1958. Theory of diffusion-limited precipitation. J. Phys. Chem. Solid 6 (4), 335–351. https://doi.org/10.1016/0022-3697(58)90053-2.
Harrer, A., Kurka, G., Warlop, R., Lasne, G., Viver, M., Resultats de l'Experience CRUSIFON 2 Compte-Rendu DMG No.61/80 (Action 4172-60)," 1980.
Harrer, A., Kurka, G., Warlop, R., Lasne, G., Viver, M., Resultats de l'Experience CRUSIFON 1 bis (dossier No.4) Compte-Rendu DMG No. 40/81 (Action 4172-60), 1981.
Higgs, J.D., Lewis, B.J., Thompson, W.T., He, Z., 2007. A conceptual model for the fuel oxidation of defective fuel. J. Nucl. Mater. 366 (1–2), 99–128. https://doi.org/10.1016/j.jnucmat.2006.12.050.
Review of Fuel Failures in Water Cooled Reactors (2006–2015) | IAEA.
Kim, K.T., 2009. The study on grid-to-rod fretting wear models for PWR fuel. Nucl. Eng. Des. 239 (12), 2820–2824. https://doi.org/10.1016/J.NUCENGDES.2009.08.018.
Killeen, J.C., Turnbull, J.A., Apr. 1987. An experimental and theoretical treatment of the release of ^{85}Kr from hyperstoichiometric uranium dioxide. In: Simpson, K.A., Wood, P. (Eds.), Proc. Workshop Chemical Reactivity of Oxide Fuel and Fission Product Release, Gloucestershire, England, Central Electricity Generating Board, 387–404.
Kim, Y.S., 2000. Fission Gas Release from U_{2+x} in Defective Fuel Rods. In: International Topical Meeting on LWR Fuel Performance, Park City, Utah, April 10–13 2000. American Nuclear Society, cf. Nucl. Tech, Taylor & Francis, pp. 9–17. https://doi.org/10.13182/NT00-A3073.
Kogai, T., 1997. Modelling of fission gas release and gaseous swelling of light water reactor fuels. J. Nucl. Mater. 244 (2), 131–140. https://doi.org/10.1016/S0022-3115(96)00731-3.
Lassmann, K., Benk, H., 2000. Numerical algorithms for intragranular fission gas release. J. Nucl. Mater. 280 (2), 127–135. https://doi.org/10.1016/S0022-3115(00)00044-1.
Lassmann, K., TRANSURANUS: a fuel rod analysis code ready for use, Nuclear Materials for Fission Reactors, pp. 295–302, 1992, doi: 10.1016/b978-0-444-89571-4.50046-3.
Lewis, B.J., 1988. Fundamental aspects of defective nuclear fuel behaviour and fission product release. J. Nucl. Mater. 160 (2–3), 201–217. https://doi.org/10.1016/0022-3115(88)90049-9.
Lewis, B.J., 1990. A generalized model for fission-product transport in the fuel-to-sheath gap of defective fuel elements. J. Nucl. Mater. 175 (3), 218–226. https://doi.org/10.1016/0022-3115(90)90210-E.
Lewis, B.J., et al., Jun. 2007. A model for predicting coolant activity behaviour for fuel-failure monitoring analysis. J. Nucl. Mater. 366 (1–2), 37–51. https://doi.org/10.1016/J.JNUCMAT.2006.11.015.
Lewis, B.J., Chan, P.K., El-Jaby, A., Iglesias, F.C., Fitchett, A., 2017. Fission product release modelling for application of fuel-failure monitoring and detection - an overview. J. Nucl. Mater. 489, 64–83. https://doi.org/10.1016/j.jnucmat.2017.03.037.
Lewis, B.J., Duncan, D.B., Phillips, C.R., 2017. Release of Iodine from Defective Fuel Elements following Reactor Shutdown 77 (3), 303–312. https://doi.org/10.13182/NT87-A33970.
Lewis, B.J., Hunt, C.E.L., Iglesias, F.C., 1990. Source term of iodine and noble gas fission products in the fuel-to-sheath gap of intact operating nuclear fuel elements. J. Nucl. Mater. 172 (2), 197–205. https://doi.org/10.1016/0022-3115(90)90438-S.
Lewis, B.J., Husain, A., 2003. Modelling the activity of ^{129}I in the primary coolant of a CANDU reactor. J. Nucl. Mater. 312 (1), 81–96. https://doi.org/10.1016/S0022-3115(02)01588-X.
Locke, D.H., 1972. The behaviour of defective reactor fuel. Nucl. Eng. Des. 21 (2), 318–330. https://doi.org/10.1016/0029-5493(72)90080-5.
Lösönen, P., 2000. On the behaviour of intragranular fission gas in UO_2 fuel. J. Nucl. Mater. 280 (1), 56–72. https://doi.org/10.1016/S0022-3115(00)00028-3.
Magni, A., et al., 2021. Chapter 8 - The TRANSURANUS fuel performance code. In: Wang, J., Li, X., Allison, C., Hohorst, J. (Eds.), Nuclear Power Plant Design and Analysis Codes. in Woodhead Publishing Series in Energy. Woodhead Publishing, pp. 161–205. https://doi.org/10.1016/B978-0-12-818190-4.00008-5.
Massih, A.R.. *2018:25* UO_2 fuel oxidation and fission gas release. https://www.stralsakerhetsmyndigheten.se/en/publications/reports/safety-at-nuclear-power-plants/2018/201825/.
Moal, A., Georgenthum, V., Marchand, O., Dec. 2014. SCANAIR: A transient fuel performance code: Part One: General modelling description. Nucl. Eng. Des. 280, 150–171. https://doi.org/10.1016/J.NUCENGDES.2014.03.055.
NINE Nuclear and Industrial Engineering.
Olander, D.R., 1976. Fundamental aspects of nuclear reactor fuel elements. Technical Lnformation Center Energy Research and Development Administration.
Olander, D.R., 1998. Mechanistic interpretations of UO_2 oxidation. J. Nucl. Mater. 252 (1–2), 121–130. https://doi.org/10.1016/S0022-3115(97)00291-2.
Olander, D.R., 2017. Oxidation of UO_2 by High-Pressure. Steam 74 (2), 215–217. https://doi.org/10.13182/NT86-A33806.
Pastore, G., Luzzi, L., Di Marcello, V., Van Uffelen, P., 2013. Physics-based modelling of fission gas swelling and release in UO_2 applied to integral fuel rod analysis. Nucl. Eng. Des. 256, 75–86. https://doi.org/10.1016/j.nucengdes.2012.12.002.
Pastore, G., Pizzocri, D., Rabiti, C., Barani, T., Van Uffelen, P., Luzzi, L., 2018. An effective numerical algorithm for intra-granular fission gas release during non-equilibrium trapping and resolution. J. Nucl. Mater. 509, 687–699. https://doi.org/10.1016/j.jnucmat.2018.07.030.
Pizzocri, D., et al., 2018. A model describing intra-granular fission gas behaviour in oxide fuel for advanced engineering tools. J. Nucl. Mater. 502, 323–330. https://doi.org/10.1016/j.jnucmat.2018.02.024.
Pizzocri, D., 2018. Modelling and assessment of inert gas behaviour in UO_2 nuclear fuel for transient analysis. Politecnico Di Milano.
Pizzocri, D., Rabiti, C., Luzzi, L., Barani, T., Van Uffelen, P., Pastore, G., 2016. PolyPole-1: an accurate numerical algorithm for intra-granular fission gas release. J. Nucl. Mater. 478, 333–342. https://doi.org/10.1016/j.jnucmat.2016.06.028.
Pizzocri, D., Barani, T., Luzzi, L., 2020. SCIANTIX: A new open source multi-scale code for fission gas behaviour modelling designed for nuclear fuel performance codes. J. Nucl. Mater. 532, 152042 https://doi.org/10.1016/j.jnucmat.2020.152042.
Politecnico di Milano. www.polimi.it.
R2CA (Reduction of Radiological Consequences of design basis and extension Accidents), 2019.
Rest, J., 2003. The effect of irradiation-induced gas-atom re-solution on grain-boundary bubble growth. J. Nucl. Mater. 321 (2–3), 305–312. https://doi.org/10.1016/S0022-3115(03)00303-9.
Rest, J., Cooper, M.W.D., Spino, J., Turnbull, J.A., Van Uffelen, P., Walker, C.T., 2019. Fission gas release from UO_2 nuclear fuel: a review. J. Nucl. Mater. 513, 310–345. https://doi.org/10.1016/j.jnucmat.2018.08.019.
Rest, J., Gehl, S.M., 1980. The mechanistic prediction of transient fission-gas release from LWR fuel. Nucl. Eng. Des. 56 (1), 233–256. https://doi.org/10.1016/0029-5493(80)90189-2.
Saad, D., Benkharfia, H., Kadouma, M., Zidi, T., 2021. Pellet-cladding mechanical interaction analysis of heavy water fuel rods under power ramps. Ann. Nucl. Energy 159, 108320. https://doi.org/10.1016/J.ANUCENE.2021.108320.
Speight, M.V., 1969. A calculation on the migration of fission gas in material exhibiting precipitation and re-solution of gas atoms under irradiation. Nucl. Sci. Eng. 37 (2), 180–185. https://doi.org/10.13182/nse69-a20676.
Tonks, M., et al., 2018. Unit mechanisms of fission gas release: Current understanding and future needs. J. Nucl. Mater. 504, 300–317. https://doi.org/10.1016/j.jnucmat.2018.03.016. Elsevier B.V.
Turnbull, J.A., 1971. The distribution of intragranular fission gas bubbles in UO_2 during irradiation. J. Nucl. Mater. 38 (2), 203–212. https://doi.org/10.1016/0022-3115(71)90044-4.
Turnbull, J.A., Beyer, C.E., 2010. Background and derivation of ANS-5.4 standard fission. Product Release Model. https://doi.org/10.2172/1033086.
Turnbull, J.A., White, R.J., Wise, C., The diffusion coefficient for fission gas atoms in uranium dioxide, in Water reactor fuel element computer modelling in steady state, transient and accident conditions, 1988, pp. 174–181.
Turnbull, J.A., Friskney, C.A., Findlay, J.R., Johnson, F.A., Walter, A.J., 1982. The diffusion coefficients of gaseous and volatile species during the irradiation of uranium dioxide. J. Nucl. Mater. 107 (2–3), 168–184. https://doi.org/10.1016/0022-3115(82)90419-6.
Turnbull, J.A., The treatment of radioactive fission gas release measurements and provision of data for development and validation of the ANS-5.4 model," OECD HALDEN REACTOR PROJECT, 2001.
Van Uffelen, P., Konings, R.J.M., Vitanza, C., Tulenko, J., Analysis of Reactor Fuel Rod Behavior, in Handbook of Nuclear Engineering, D. G. Cacuci, Ed., 1st ed.Springer US, 2010.

Van Uffelen, P., Pastore, G., Di Marcello, V., Luzzi, L., 2011. Multiscale modelling for the fission gas behaviour in the TRANSURANUS Code. Nucl. Eng. Technol. 43 (6), 477–488. https://doi.org/10.5516/NET.2011.43.6.477.

Verma, L., Noirot, L., Maugis, P., A new spatially resolved model for defects and fission gas bubbles interaction at the mesoscale, Nucl Instrum Methods Phys Res B, vol. 458, no. October 2018, pp. 151–158, 2019, doi: 10.1016/j.nimb.2018.10.028.

Verma, L., Noirot, L., Maugis, P., 2020. Modelling intra-granular bubble movement and fission gas release during post-irradiation annealing of UO_2 using a meso-scale and spatialized approach. J. Nucl. Mater. 528, 151874 https://doi.org/10.1016/j.jnucmat.2019.151874.

Veshchunov, M.S., 2008. Modelling of grain face bubbles coalescence in irradiated UO_2 fuel. J. Nucl. Mater. 374 (1–2), 44–53. https://doi.org/10.1016/j.jnucmat.2007.06.021.

Veshchunov, M.S., 2019. Mechanisms of fission gas release from defective fuel rods to water coolant during steady-state operation of nuclear power reactors. Nucl. Eng. Des. 343, 57–62. https://doi.org/10.1016/J.NUCENGDES.2018.12.021.

Veshchunov, M.S., Tarasov, V.I., Jun. 2013. Modelling of irradiated UO_2 fuel behaviour under transient conditions. J. Nucl. Mater. 437 (1–3), 250–260. https://doi.org/10.1016/j.jnucmat.2013.02.011.

Vitanza, C., Kolstad, E., Graziani, U., 1979. Fission gas release from UO_2 pellet fuel at high burn-up, OECD HALDEN REACTOR PROJECT, pp. 361–366.

White, R.J., 2004. The development of grain-face porosity in irradiated oxide fuel. J. Nucl. Mater. 325 (1), 61–77. https://doi.org/10.1016/j.jnucmat.2003.10.008.

White, R.J.J., Corcoran, R.C.C., Barnes, R.S., Barnes, P.J., A Summary of Swelling Data Obtained from the AGR/Halden Ramp Test Programme, R&T/NG/EXT/REP/0206/02, no. 5, pp. 1–192, 2006.

White, R.J., Tucker, M.O., 1983. A new fission-gas release model. J. Nucl. Mater. 118 (1), 1–38. https://doi.org/10.1016/0022-3115(83)90176-9.

Yang-Hyun, K., Dong-Seong, S., Young-Ku, Y., 1994. An analysis method for the fuel rod gap inventory of unstable fission products during steady-state operation. J. Nucl. Mater. 209 (1), 62–78. https://doi.org/10.1016/0022-3115(94)90248-8.

Zullo, G., Pizzocri, D., Luzzi, L., 2022a. On the use of spectral algorithms for the prediction of short-lived volatile fission product release: Methodology for bounding numerical error. Nucl. Eng. Technol. 54 (4), 1195–1205. https://doi.org/10.1016/J.NET.2021.10.028.

Zullo, G., Pizzocri, D., Magni, A., Van Uffelen, P., Schubert, A., Luzzi, L., 2022b. Towards grain-scale modelling of the release of radioactive fission gas from oxide fuel. Part I: SCIANTIX. Nuclear Eng. Technol. https://doi.org/10.1016/J.NET.2022.02.011.

Zullo, G., Pizzocri, D., Magni, A., Van Uffelen, P., Schubert, A., Luzzi, L., 2022c. Towards grain-scale modelling of the release of radioactive fission gas from oxide fuel. Part II: Coupling SCIANTIX with TRANSURANUS. Nucl. Eng. Technol. 54 (12), 4460–4473. https://doi.org/10.1016/J.NET.2022.07.018.

Zullo, G., Pizzocri, D., Luzzi, L., Kremer, F., Arnold, N., Muellner, N., Zimmerl, R., Klouzal, J., Gumenyuk, D., Herranz, L. E., Iglesias, R., Cherubini, M., Giaccardi, L., Schubert, A., Van Uffelen, P., Bürger, B., Hózer, Z., 2023a. Final report on rod cladding failure during SGTR, pp. 1–65. Available: https://re.public.polimi.it/handle/11311/1233279.

Zullo, G., Pizzocri, D., Luzzi, L., Kremer, F., Dubourg, R., Schubert, A., Van Uffelen, P., 2023b. Towards simulations of fuel rod behaviour during severe accidents by coupling TRANSURANUS with SCIANTIX and MFPR-F. Ann. Nucl. Energy 190, 109891. https://doi.org/10.1016/J.ANUCENE.2023.109891.

Zullo, G., Pizzocri, D., Luzzi, L., 2023c. The SCIANTIX code for fission gas behaviour: Status, upgrades, separate-effect validation, and future developments. J. Nucl. Mater. 587, 154744. https://doi.org/10.1016/J.JNUCMAT.2023.154744.